

Article

Belief Reliability Modeling Method for Wind Farms Considering Two-Directional Rotor Equivalent Wind Speed

Shuyu Li ^{1,2}, Rui Kang ^{1,2} , Meilin Wen ^{2,*} and Tianpei Zu ^{1,2}

¹ Hangzhou International Innovation Institute, Beihang University, Hangzhou 311115, China; lishuyu@buaa.edu.cn (S.L.); kangrui@buaa.edu.cn (R.K.); zutp93@buaa.edu.cn (T.Z.)

² School of Reliability and Systems Engineering, Beihang University, Beijing 100191, China

* Correspondence: wenmeilin@buaa.edu.cn

Abstract: Compared to conventional energy sources, wind power is a clean energy source with high intermittence and uncertainty. As a system that converts wind energy into electricity, wind farms inevitably face severe reliability issues. In this paper, based on reliability theory, a new reliability modeling method for wind farms is proposed. Firstly, a belief reliability model for wind farms is constructed. Then, a power generation model based on two-directional rotor equivalent wind speed is established to represent the wind farm performance in the belief reliability model. Finally, several numerical studies are conducted to verify the power generation model under different wind speeds and directions, to demonstrate the belief reliability model with different levels of uncertainty, and to compare the belief reliability considering two-directional rotor equivalent wind speed with other methods.

Keywords: reliability model; belief reliability; rotor equivalent wind speed; wind farm



Citation: Li, S.; Kang, R.; Wen, M.; Zu, T. Belief Reliability Modeling Method for Wind Farms Considering Two-Directional Rotor Equivalent Wind Speed. *Symmetry* **2024**, *16*, 614. <https://doi.org/10.3390/sym16050614>

Academic Editor: Calogero Vetro

Received: 19 March 2024

Revised: 7 May 2024

Accepted: 10 May 2024

Published: 15 May 2024



Copyright: © 2024 by the authors. Licensee MDPI, Basel, Switzerland. This article is an open access article distributed under the terms and conditions of the Creative Commons Attribution (CC BY) license (<https://creativecommons.org/licenses/by/4.0/>).

1. Introduction

The energy crisis and environmental pollution are major issues around the world, and accelerating the development of clean energy is the trend of sustainable development. As an important renewable energy, wind has been increasingly considered due to its clean, safe, and large reserves. Wind power generation has also received widespread attention from countries around the world. The Global Wind Energy Council (GWEC) released the 2023 Global Wind Energy Report [1], which states that in 2022, the world's newly installed wind power capacity was 77.6 GW, with a cumulative capacity of 906 GW, an increase of 9% compared to 2021. Meanwhile, the report predicts that the cumulative installed capacity of global wind power will increase to 1586 GW over the next five years (2023–2027) under existing policies, with a very optimistic outlook.

Reliability issues relating to wind farms (WFs) have also emerged. In contrast to traditional power generation methods under steady-state conditions, wind energy is characterized by fluctuation, variation and intermittency. This results in wind turbines operating under non-stationary loads in highly stochastic environments, which introduces significant uncertainty. Much research has begun to focus on the reliability of WFs.

Some studies [2–4] applied traditional reliability metrics to wind turbines (WTs), such as failure rate, Mean Time Between Failures (MTTF), Mean Time To Repair (MTTR), and availability to obtain WF reliability through analytical or simulation methods. The analytical methods [5,6] derive the analytical model of WF reliability through the probability expression of the state of WTs. The simulation methods [7] mainly adopt Monte Carlo simulation, which samples the wind speed and the states of WTs to statistically obtain the reliability results. However, the reliability of WFs is mainly evaluated by reliability indices directly related to the performance of power generation, such as Duration per Interruption (D) [8,9], Load Not Supplied per Interruption (LNSI) [8,9], Energy Not Supplied Interruption (ENSI) [8,9] and other deterministic indices, as well as expected energy

not supplied (EENS) [4,10], Loss of Load Expectation (LOLE) [2–4,8,10], Loss of Energy Expectation (LOEE) [3,8], Expected Available Wind Energy (EAWWE) [11], Expected Generated Wind Energy (EGWE) [11], capacity factor (CF) [8,11], and other indices obtained by expected values, probabilities, and frequencies.

These performance–evaluation-type reliability indices are widely used in the reliability practice of WFs since there are mostly decreases in power generation capacity and almost no system failures for WFs. However, reliability is generally defined as the capability of a component or a system to perform a specified function for a given period of time under stated operating conditions. Existing WF reliability models corresponding to the performance–evaluation-type reliability indices are not completely compatible with the definition of reliability.

Therefore, to better balance the practical needs and the scientific rigor that matches the definition of WF reliability, an effective reliability analysis and modeling method is urgently needed. Belief reliability is a new reliability metric proposed by Kang [12] to describe the reliability of components or systems affected by uncertainty. It focuses on evaluating reliability by using the difference between a system's performance margin and its threshold under uncertainty, without components' failure rate, state transition probability, or any other failure-related information. Thus, it is suitable for modeling the reliability of wind farms from the perspective of power generation. Modeling wind farm reliability based on belief reliability theory can distinguish different wind turbines in a wind farm and consider their spatial mutual interference, establish the relationship between performance parameters and power generation, and quantify the uncertainty of the wind farm. Belief reliability theory has been employed in analyzing the reliability of multi-state deteriorating systems [13], the lock mechanism of the aircraft landing gear door [14], and in modeling reliability for two-phase degradation systems [15], software systems [16,17], urban road traffic [18], and radar [19]. To the best of our knowledge, there is no research using belief reliability theory to model the reliability of wind farms. Therefore, based on belief reliability theory, we propose a wind farm reliability modeling method.

Wind farm belief reliability modeling relies on accurate wind farm power generation results. The traditional method uses the hub height wind speed (HHWS) to calculate power generation; that is, the wind speed of the hub center is the speed of the wind turbine. With technological advancements, the diameter of wind turbines continues to increase. Thus, without considering the influence of wind shear, there is significant differences in power generation based on hub height wind speed compared to actual values [20]. Considering the variation of wind speed in the vertical direction of wind turbines, some scholars believe that HHWS cannot fully represent the wind speed of the entire wind turbines. Therefore, the study of wind shear has been the focus of many researchers, and the rotor equivalent wind speed (REWS) has been proposed as the method of calculating the effect of wind shear on rotor wind speed. Based on the equivalent wind speed formulation proposed by Wagner et al. [20], Choukulkar et al. [21] proposed a new formula considering the effects of wind speed direction fluctuations, wind shear, wind speed turbulence, and directional shear to calculate the equivalent wind power. Scheurich et al. [22] compared the annual energy production estimated using the HHWS and REWS power curve, and pointed out that REWS could result in more accurate predictions of the annual energy production (AEP) of a turbine. Jeon et al. [23] applied REWS to predict the AEP of a wind turbine and demonstrated the need for using REWS by comparing the error percentages. Redfern et al. [24] implemented the REWS in the Weather Research and Forecasting (WRF) Model and found out that for scenarios with highly nonlinear wind shear, REWS is much more appropriate. The study of Ryu et al. [25] showed that, in most cases, power production calculated using the REWS is closer to the actual power output than that calculated using the HHWS.

Although the REWS is better than the HHWS in representing the wind speed over the entire plane of wind wheel rotation, REWS is imperfect. It only considers the variation of wind speed in the vertical direction (i.e., wind shear), using a certain wind speed to

represent the wind speed at all positions within that height layer on the wind wheel rotation plane, without considering the variation of wind speed in the horizontal direction. However, under the influence of wake effects, the wind speed at different horizontal directions within the same height layer may be quite different. For example, there is a situation where the downwind wheel rotation plane is partially affected by the wake and partially unaffected. The influence of wake within the same height layer will decrease to zero as the distance from the upwind wake center increases, and the wind speed will correspondingly increase until no reduction occurs. Therefore, considering the variation of wind speed on the height and the width of the wind turbine, we propose a two-directional rotor equivalent wind speed (2D-REWS) model to calculate the wind generation for wind farm belief reliability modeling.

This paper is organized as follows. Section 2 provides some preliminaries on the belief reliability theory and the three-dimensional Jensen–Gaussian wake model. The wind farm belief reliability model and the power generation model based on 2D-REWS are introduced in Sections 3 and 4, respectively. In Section 5, two numerical examples are employed to demonstrate the proposed method. Section 6 concludes this paper.

2. Preliminaries

Some basic concepts of belief reliability theory and a three-dimensional Jensen–Gaussian (3DJG) wake model are introduced in this section, which are used to deduce the mathematical model of the proposed method in this paper.

2.1. Belief Reliability Theory

Belief reliability is a new reliability metric proposed by Kang [12], which builds a theoretical discourse of reliability expressed via a margin equation, degradation equation and metric equation based on some basic definitions and principles. Reliability is the ability of a product to perform a specified function within a specified time under specified conditions. To describe this meaning clearly, the theory of belief reliability introduces the concepts of the state variable and the feasibility domain. The state variable is a set of variables that describe the behavior of a product, and the feasibility domain is the space of values of the state variable that allow a product not to completely lose its function. If the state variable is in the feasible domain, it means that the product works. The state variables describe the behavior of the product, and the feasibility domain reflects the criterion of functional feasibility. The failure behavior of the product is actually caused by the failure of the functional behavior, which is the ultimate expression of the functional behavior, so the core state variable is the variable that can describe the functional behavior. Functionality reflects human needs for the product, which can be represented by one or more specific performance parameters, and whether the product can perform the specified function depends on how much performance margin is provided for the function. Therefore, the basic principles of reliability theory are as follows:

Principle 1 Margin-based Reliable Principle: The performance margin determines how reliable the object is.

Principle 2 Eternal Degradation Principle: The object performance margin undergoes irreversible degradation along the time vector.

Principle 3 Uncertainty Principle: The object performance margin and its degradation process are uncertain.

The related definitions of belief reliability, performance margin, and performance threshold of requirements are as follows.

Definition 1. *Belief reliability: Assume that the state variable of a system ξ is an uncertain random variable whose reliable domain is Ξ . The belief reliability of this system is defined as the chance that the state variable is in the reliable domain, that is*

$$R_B = \Pr\{\xi \in \Xi\}. \quad (1)$$

Definition 2. *Performance Threshold of Requirements:* The requirements of the subject for the specified function of the object.

Definition 3. *Performance Margin:* The performance margin represents the distance between the performance parameter and the performance threshold of requirements, which can be written as a margin equation

$$\mathbf{M} = m_{\vec{t}}(\mathbf{P}, \mathbf{P}_{\text{th}}), \quad (2)$$

where \mathbf{P} is the performance parameter vector, and \mathbf{P}_{th} is the performance threshold of the requirement vector.

Based on the reliability principle of margin and uncertainty, the performance margin determines how reliable the object is, and the object's performance margin is uncertain. Thus, when the state variable is referred to as the performance margin, the belief reliability function of the performance margin can be written as a metric equation:

$$R_B = \Pr\{\tilde{\mathbf{M}} > 0\}, \quad (3)$$

The performance parameters are derived from the physical laws of various fields, which can be written as an interdisciplinary equation:

$$\mathbf{P} = g_{\vec{t}=0}(\mathbf{X}, \mathbf{Y}, t), \quad (4)$$

where \mathbf{X} and \mathbf{Y} are the vectors of internal and external parameters, respectively, and t is the time vector.

2.2. Three-Dimensional Jensen-Gaussian (3DJG) Wake Model

The 3DJG model [26] is a wake model considering the wind shear and turbulence intensity on wake recovery rate based on the Jensen model using a Gaussian distribution. Some important wind speed equations are as follows.

With the hub center of the wind turbine as the coordinate origin, the horizontal velocity distribution at arbitrary height z and at the radial position y at the horizontal level at the downwind position x in the wake region is

$$u(x, y, z) = u_{\text{ref}} \cdot \left(\frac{z + z_{\text{hub}}}{z_{\text{ref}}} \right)^\alpha - \frac{\zeta}{\sigma_y \sqrt{2\pi}} e^{-\frac{y^2}{2\sigma_y^2}}, \quad (5)$$

where u_{ref} is the incoming wind speed measured at a reference height z_{ref} (m/s), $z + z_{\text{hub}}$ is the absolute height above ground (m), α is the wind shear index, σ_y is decided by $r_y = 2.58\sigma_y = k_y x + r_0$ (m), and k_y represents the wake expansion coefficient in the horizontal plane.

ζ is the speed distribution in the vertical direction (m/s):

$$u(x, z) = u_0(x, z) + \Delta u - \frac{\int_{-r_0}^{r_0} (\Delta u \times a) dz}{r_z}, \quad (6)$$

where

$$u_0(x, z) = u_{\text{ref}} \cdot \left(\frac{z_{\text{hub}}}{z_{\text{ref}}} \right)^\alpha - \frac{4ar_0^2 u_{\text{ref}} \cdot \left(\frac{z_{\text{hub}}}{z_{\text{ref}}} \right)^\alpha}{r_z \sigma_z \sqrt{2\pi}} e^{-\frac{z^2}{2\sigma_z^2}}, \quad (7)$$

and

$$\Delta u = u(z) - u(z_{\text{hub}}), \quad (8)$$

where the axial induction factor is $a = (1 - \sqrt{1 - C_T})/2$, C_T is the thrust coefficient, the initial wake radius $r_0 = R\sqrt{(1-a)/(1-2a)}$ (m), and the wake radius is $r_z(x) = 2.58\sigma_z = k_z x + r_0$ (m).

3. Belief Reliability Model for Wind Farm

Reliability is defined as the ability to perform a specified function within a specified period of time under a specified condition. For wind farms, their function is to ensure that the power generation meets its demand and to avoid mismatch at the medium-to-long-term scale. Wind farm reliability refers to the ability of a wind farm to match its power generation with the demand. Based on belief reliability theory, we propose wind farm belief reliability, build the wind farm margin equation, and measure the uncertainty.

3.1. Description of Wind Farm

A wind farm, denoted by WF, is the system that arranges multiple wind turbines in an area with good wind energy resources to generate power in a certain layout. The research object of this paper focuses on the wind farm systems composed of multiple wind turbines, whose power generation is influenced by the layout, as well as external meteorological and geographical factors. The wind farm systems do not include the transmission electronic systems, the control subsystems, the network monitoring systems, and the energy storage devices.

The total number of wind turbine subsystems in the wind farm is N , and each wind turbine is a subsystem of WF, denoted by WT_n , that satisfies $WT_n \subset WF, n = 1, 2, \dots, N$.

3.1.1. Wind Farm Layout

The layout is the spatial arrangement of wind turbines in a wind farm. For the layout of wind farm systems in this paper, there are two representation methods. One is the absolute position coordinate system, and it is used to input the layout of the wind farms, and the other is the relative position coordinate system, which is used for calculating the power of wind farms in different wind directions. The two-coordinate system sometimes requires mutual conversion; here, an example to illustrate the conversion process is shown.

Example 1. Coordinate systems of the wind farm and their conversion:

As shown in Figure 1, in this example, we adopt the right-hand coordinate system $O - XYZ$ as the absolute position coordinate system of the wind farm, and the position coordinate of the wheel hub height of the wind turbine WT_n is (x_n, y_n, z_n) . The coordinates are in meters.

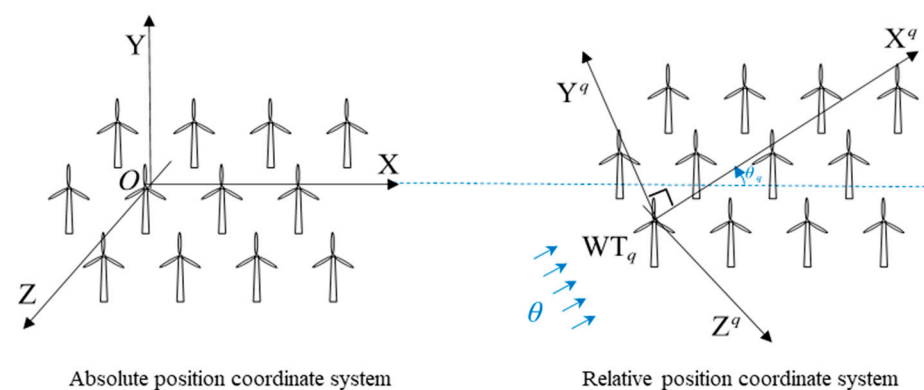


Figure 1. Coordinate systems of the wind farm layout.

Under the wind direction θ , a new right-handed coordinate system was established. The hub height center of WT_q is taken as the coordinate origin, the downwind direction is designated as the positive direction of X^q axis, and the Y^q axis is designated as a rotation of 90° counterclockwise perpendicular to the downwind direction. The coordinate system of the wind farm was called the relative position coordinate system marked as $\theta - q$.

At this time, the angle between the X^q axis and the X axis is θ_q (counterclockwise is positive), then the coordinates of each WT_n at the hub height under the absolute coordinate

system (x_n, y_n, z_n) are transformed to the coordinates (x_n^q, y_n^q, z_n^q) under the $\theta - q$ relative position coordinate system. The coordinates (x_n^q, y_n^q, z_n^q) are as follows:

$$x_n^q = (x_n - x_q) \cos \theta_q + (y_n - y_q) \sin \theta_q, \quad (9)$$

$$y_n^q = (y_n - y_q) \cos \theta_q - (x_n - x_q) \sin \theta_q, \quad (10)$$

$$z_n^q = z_n - z_q. \quad (11)$$

3.1.2. Wind Farm Interference Relationship

The interference relationship of a wind farm refers to the influences formed by the wake effect between wind turbines within the wind farm area. To describe the interference relationship between wind turbines, three necessary definitions are given in this paper.

Definition 4. *Upwind Turbine:* Let the relative position coordinate system established with any wind turbine numbered q . For any $WT_{n_1}^q$ and $WT_{n_2}^q$ ($n_1 < n_2$), if their coordinates satisfy $x_{n_1}^q \leq x_{n_2}^q$, then the $WT_{n_1}^q$ is said to be the upwind turbine of $WT_{n_2}^q$; otherwise, the $WT_{n_2}^q$ is said to be the upwind turbine of $WT_{n_1}^q$.

Definition 5. *The Most Upwind Turbine:* Let the relative position coordinate system established with any wind turbine numbered q , for all wind turbines WT_n^q , if (1) WT_s^q satisfies: $\forall n, x_s^q \leq x_n^q$, then the WT_s^q is considered to be the most upstream turbines. (2) WT_s^q satisfies: $s = \min\{S_\lambda\}$ and $x_{S_\lambda}^q \leq x_n^q$, when there are multiple turbines $WT_{S_\lambda}^q$ ($\lambda = 1, 2, \dots, \Lambda$) and $x_{S_1}^q = x_{S_2}^q = \dots = x_{S_\Lambda}^q$, the turbine WT_n^s with the smallest serial number is considered to be the most upstream turbine.

Definition 6. *The Bidirectional interference Relationship Matrix:* The bidirectional interference relation matrix W of the wind farm is a matrix of $N \times N$, and each element w_{ij}^s represents whether there is an interference relationship between wind turbine WT_i^s and WT_j^s in the coordinate system with the most upwind turbine WT_s^s as the origin, as follows:

$$w_{ij}^s = \begin{cases} 1, & \text{if } j \in \Gamma_i^s \\ 0, & \text{if } i, j \notin \Gamma_j^s \\ -1, & \text{if } i \in \Gamma_j^s \end{cases} \quad (12)$$

where Γ_i^s represents the wind turbine set affected by wind turbine WT_i^s in the coordinate system with the most upwind turbine WT_s^s as the origin.

3.2. Belief Reliability Analysis of Wind Farm

Different from traditional reliability modeling and analysis methods, the belief reliability analysis method uses a margin equation to describe the degree to which the functions and performance of wind farms meet the requirements, that is, the reliability degree, and the metric equation is used to describe the influence of uncertainty on the reliability degree of the system. The former is the part used to obtain the reliability certainty of wind farm systems, and the latter is the influence of uncertainty during the process of completing the function. Both jointly complete the analysis of wind farm reliability. Therefore, this section describes the belief reliability analysis method based on the margin equation and measurement equation of wind farms.

3.2.1. Wind Farm Margin Equation

According to the Margin-based Reliable Principle [12], the performance margin determines how reliable the object is. The normal status is that the margin of the system

output performance is greater than zero. When the margin of performance is less than or equal to zero, the system is in the failure status. According to Definition 3, the system's performance margin is characterized by its performance parameters and the corresponding performance threshold. The system's performance, which includes aspects such as motor output torque, battery capacity, and gear ratio, is an external manifestation of its functions. In line with the definition of reliability, the system's performance parameters should be capable of describing the execution of the system's fixed functions. Performance thresholds, on the other hand, set limits on the performance parameters associated with these functions. For wind farms, the most important function is to convert wind energy into electricity, the corresponding performance parameter is the power generation, and the performance threshold is the demand for power generation. The performance margin of wind farm M_{WF} is the distance between power generation and its requirement:

$$M_{\text{match}} = m(E_{WF}(\mathbf{X}, \mathbf{Y}, t), E_{\text{th}}), \quad (13)$$

where E_{WF} is the power generation, and E_{th} is the requirement of wind farm power generation.

In the context of a wind farm system, the normal operational state is characterized by power generation exceeding the demand for power. Obviously, the power generation belongs to the larger-the-better performance parameter, and the greater the power generation exceeds the power demand, the larger the performance margin. Therefore, the distance function can be used to describe the relatively simple Euclidean distance description that can describe the desired performance, so the performance margin of a wind farm can be described as follows:

$$M_{\text{match}} = E_{WF}(\mathbf{X}, \mathbf{Y}, t) - E_{\text{th}}. \quad (14)$$

This equation can ensure that when the power generation is greater than the power generation demand value, the performance margin is greater than 0, and the greater the power generation, the greater the performance margin.

3.2.2. Wind Farm Uncertainty Measurement

In practice, wind farms face various uncertainties, which may render them unreliable despite having sufficient margins. Therefore, to enhance the reliability assessment of wind farms, it is imperative to first analyze and quantify these uncertainties.

External uncertainty is the main source of uncertainty in wind farms. The working environment of wind farms is complex and variable, thus there are fluctuations and changes in related parameters such as meteorological conditions and geographical environment. These factors can have an impact on the margin of wind farms. Among those external parameters \mathbf{Y} , wind speed v , which serves as the input for wind farm power generation, is the main factor. Thus, in this paper, we consider the uncertainty of wind speed.

For a given wind distribution, wind speed $v = (v_1, v_2, \dots, v_K)$ is regarded as a multi-dimensional random variable and follows a multidimensional normal distribution:

$$v \sim N(\boldsymbol{\mu}, \boldsymbol{\Sigma}), \quad (15)$$

where $\boldsymbol{\mu} = (\mu_1, \mu_2, \dots, \mu_K)$, $\boldsymbol{\Sigma} = [\Sigma_{ij}]$, $\Sigma_{ij} = \text{Cov}(v_i, v_j)$.

3.2.3. Wind Farm Metric Equation

Given that wind speed directly influences the power generation of wind farms, the uncertainty associated with wind speed propagates to the performance parameters of the wind farms, which, in turn, causes the performance margin to have a distribution. According to the Uncertainty Principle [12], the performance margin greater than 0 means that the system is reliable, and the reliability of the wind farm is expressed as the probability that the performance margin of the system is greater than 0.

According to the Definition 1, the metric equation of wind farm belief reliability is

$$R_B = \Pr(\tilde{M}_{WF} > 0), \quad (16)$$

where R_B is belief reliability, and \tilde{M}_{WF} is the wind farm performance margin considered uncertain. The expression for reliability can be further obtained as follows:

$$\begin{aligned} R_B &= \Pr(\tilde{M}_{WF}(v) > 0) \\ &= 1 - \Phi_{M_{WF}(v)}(0), \end{aligned} \quad (17)$$

where $\Phi_{M_{WF}(v)}$ represents the distribution function of the performance margin \tilde{M}_{WF} , which is related to the distribution function of wind speed, and the specific relationship is determined by the functional relationship between wind speed and power generation, which is referred to in Section 4.

From Equation (16), it is evident that the metric equation of belief reliability can be used to evaluate a system's reliability by integrating the uncertainties inherent in the system into the system performance margins. This approach significantly deviates from traditional reliability methods, which necessitate the input of component failure rates or state transition probabilities. This unique feature endows the belief reliability assessment method proposed in this paper for wind farms with the capability to be applied throughout the entire life cycle of the system, eliminating the need to acquire statistical information, such as component failure rates.

4. Power Generation Model Based on Two-Directional Rotor Equivalent Wind Speed

Drawing upon belief reliability theory, the first step in modeling the reliability of a wind farm involves establishing interdisciplinary equations for the performance parameters. Over an extended time scale, power generation is typically used as the primary indicator of wind farm performance. To account for the variation of wind speed across both the height and width of the wind turbine, we propose a power generation model based on two-dimensional rotor equivalent wind speed (2D-REWS).

4.1. Two-Directional Rotor Equivalent Wind Speed (2D-REWS) Model

In recent years, with increased wind turbine diameter, the concept of rotor equivalent wind speed (REWS) considering wind shear has been proposed, and the IEC 61400-12-1 standard (2nd revised in 2017) [27] also calculates the equivalent wind speed of a wind turbine by measuring the wind speed at multiple heights within the wind turbine. This is carried out to evaluate the power of the wind turbine. The equivalent wind speed of a wind turbine is defined as follows:

$$v_{eq} = \sqrt[3]{\sum_i \frac{A_i v_i^3}{A}}, \quad (18)$$

where i is the number of each layer divided by the height of the wind turbine, v_i is the wind speed at different heights of the wind turbine (m/s), A_i is the area of the wind turbine rotor at the corresponding height of v_i (m^2), and $A = \pi R^2$ is the area of a wind turbine rotor (m^2).

Based on the equivalent wind speed of the wind turbine, this paper not only considers the variation of wind speed on the height of the wind turbine but also that on the width of the wind turbine. In combination with a three-dimensional wake model considering wind shear, a two-directional rotor equivalent wind speed (2D-REWS) and its calculation method for wind turbines affected by wake effects are proposed. The specific approach involves using the concept of double integration along the height (m) and width of the

wind turbine rotor (m), and the wind speed (m/s) at each position on the rotor of a wind turbine can be equivalent to the height of the hub:

$$v_{eq,i}^{s,j} = \sqrt{\frac{\int_{y_i^s-R_i}^{y_i^s+R_i} \left[\int_{z_i^s-\sqrt{R_i^2-(y^s-y_i^s)^2}}^{z_i^s+\sqrt{R_i^2-(y^s-y_i^s)^2}} v_s^3(x_i^s, y^s, z^s) dz^s \right] dy^s}{A}}, \quad (19)$$

or

$$v_{eq,i}^{s,j} = \sqrt{\frac{\int_{z_i^s-R_i}^{z_i^s+R_i} \left[\int_{y_i^s-\sqrt{R_i^2-(z^s-z_i^s)^2}}^{y_i^s+\sqrt{R_i^2-(z^s-z_i^s)^2}} v_s^3(x_i^s, y^s, z^s) dy^s \right] dz^s}{A}}. \quad (20)$$

In practice, the above process can be discretized and divided into multiple grids along the height and width of the rotor of wind turbine, as shown in Figure 2. The coordinates of each grid's center point represent the wind speed within that grid, and then equivalent calculations can be performed.

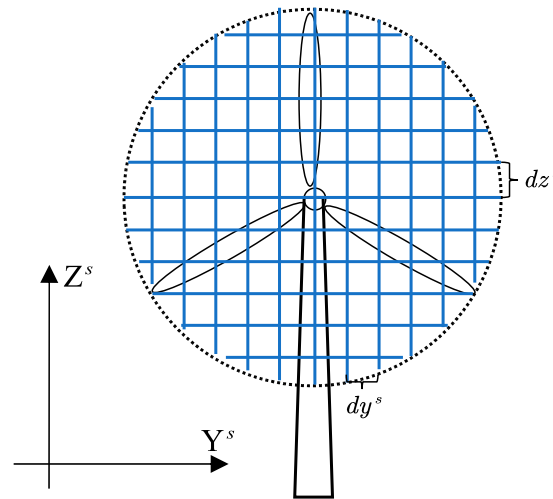


Figure 2. Discretization method diagram to calculate 2D-REWS.

4.2. Wind Farm Power Generation Affected by Multiple Wakes

In practice, wake effects have a significant impact on the output power of wind farms. According to research, the power generation loss caused by wake effects is generally 5% to 15%, sometimes even up to 30% to 40% [28,29]. Furthermore, a wind farm usually comprises more than one wind turbine, with each downstream wind turbine potentially being affected by multiple upstream wind turbines. Therefore, it is essential to consider the influence of multiple wind turbines. Consequently, in accordance with the 2D-REWS model we proposed, we adopted a three-dimensional Jensen–Gaussian (3DJG) wake model and considered the impact of multiple wakes to construct a wind farm power generation model.

Considering any position (x^s, y^s, z^s) in the wind farm, as shown in Figure 3, the yellow area represents the wake area of wind turbine WT_j , and the cross-section at the downwind position x^s is a circle with the radius $r_{z_j}(x^s - x_j^s)$.

When position (x^s, y^s, z^s) is on and inside the circle, it will be affected by wake, and the wind speed follows Equation (5). When position (x^s, y^s, z^s) is outside the circle, it will not be affected by wake, and the wind speed can be expressed as the logarithmic wind profile:

$$u_0(z^s) = u_{ref} \frac{\ln((z^s + z_s^s)/z_0)}{\ln(z_{ref}^s/z_0)}, \quad (21)$$

where z_j^s is the vertical coordinates of WT_j (m).

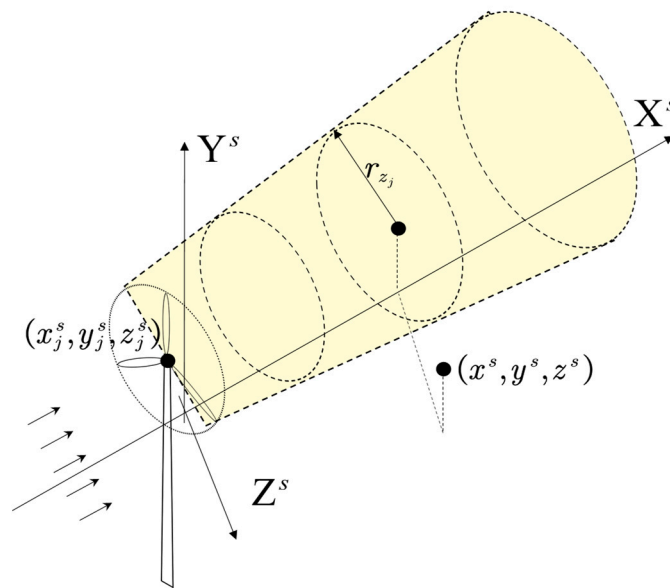


Figure 3. Diagram of wake effect in wind farm.

Therefore, in the coordinate system with wind turbine WT_j as the origin, the wind speed at location (x^s, y^s, z^s) that is only affected by WT_j can be expressed as a piecewise function:

$$v(x^s, y^s, z^s) = \begin{cases} u(x^s - x_j^s, y^s - y_j^s, z^s - z_j^s), & \text{if } \sqrt{(y^s - y_j^s)^2 + (z^s - z_j^s)^2} \leq r_{zj}(x^s - x_j^s) \\ u_0(z^s), & \text{else} \end{cases} \quad (22)$$

To determine the wind speed of downwind turbines affected by a single upwind turbine, it is essential to construct an interference relationship matrix for the wind farms. This matrix will facilitate the determination of the interference relationship between wind turbines. The specific process is as follows:

The positional relationship between the upwind turbine wake circle and the rotor circle of the downwind turbine is crucial when constructing the interference relationship matrix. This positional relationship can include five kinds: external separation, external tangent, intersection, internal tangent, and inclusive, as shown in Figure 4.

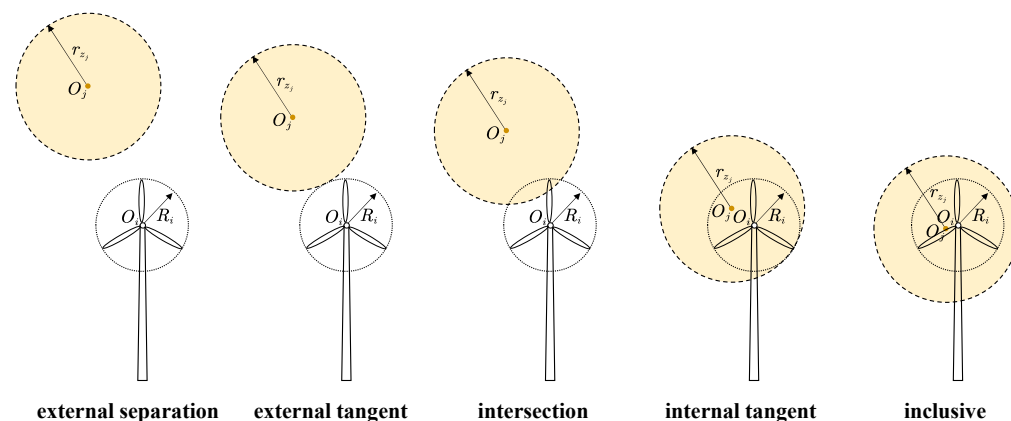


Figure 4. Relation between the upwind turbine wake circle and the rotor circle of downwind turbine.

The downwind turbine is influenced by the wake of the upwind turbine when the two circles are at the last four different positional relationships: external tangent, intersection,

internal tangent, or inclusion. According to the positional relationship between the two circles, the set of wind turbines Γ_j^s , which are affected by the upwind turbine WT_j , can be defined as follows:

$$\Gamma_j^s = \left\{ i \neq j \mid \sqrt{(y_j^s - y_i^s)^2 + (z_j^s - z_i^s)^2} \leq r_{z_j}(x_i^s - x_j^s) + R_i \right\}. \quad (23)$$

where $r_{z_j}(x_i^s - x_j^s)$ is the wake radius of upwind turbine WT_j at the downwind position x_i^s , and R_i is the wind turbine radius of downwind turbine WT_i .

Further, we adopt an energy balance (EB) method to calculate the wind speed under the interaction of multiple wind turbine wakes. In the coordinate system with wind turbine WT_s as the origin, the wind speed of WT_i affected by the wake of J wind turbines can be expressed as follows:

$$v_{eq,i}^s = \sqrt{v_0^2 - \sum_{j=1}^J (v_{eq,j}^s)^2 - v_{eq,i}^s{}^2}, \quad (24)$$

where v_0 is the incoming wind speed (m/s), $v_{eq,j}^s$ is the 2D-REWS of WT_j (m/s), $v_{eq,i}^s$ is the 2D-REWS of WT_i only affected by WT_j (m/s).

Then, the power curve of wind turbine WT_n is as follows:

$$p_n(v_{eq,n}) = \begin{cases} 0 & 0 \leq v_{eq,n} < v_{in,n}, v_{eq,n} > v_{out,n} \\ \frac{1}{2} \rho \pi R^2 C_{p,n} \cdot v_{eq,n}^3 & v_{in,n} \leq v_{eq,n} < v_{r,n} \\ p_{r,n} & v_{r,n} \leq v_{eq,n} < v_{out,n} \end{cases}, \quad (25)$$

where ρ is the air density (kg/m^3), $C_{p,n}$ is the power coefficient of WT_n , $v_{eq,n}$ is the 2D-REWS of WT_n affected by multiple wake (m/s), $p_{r,n}$ is the rated power of WT_n (kW), $v_{in,n}$ is the cut-in wind speed of WT_n (m/s), $v_{r,n}$ is the rated wind speed of WT_n (m/s), and $v_{out,n}$ is the cut-out wind speed of WT_n (m/s).

The power generation of a wind farm is the sum of the power generation of all wind turbines:

$$E_{WF} = \sum_{n=1}^N \int p_n(v_{eq,n}) f(v_{eq,n}) dv_{eq,n} \cdot t, \quad (26)$$

where $f(v_{eq,n})$ is the wind distribution of $v_{eq,n}$, E_{WF} is the power generation of a wind farm (kWh), and t is the power generation time (h).

5. Numerical Examples

Two sets of numerical examples are presented in this section to better illustrate the belief reliability modeling method we proposed. The first set of example shows the changes in wind farm power generation under different wind speeds and directions, and the second provides belief reliability results under conditions of varying degrees of wind speed uncertainty. All the results presented in this section were calculated in MATLAB R2021b.

5.1. Power of Wind Farm under Different Wind Speeds and Directions

To verify the power generation model of wind farms based on the 2D-REWS model, we performed calculations and analyses of wind farm power under varying wind speeds and directions.

In the numerical examples used in this section, the wind farm is composed of nine wind turbines, and the layout is given as shown in Figure 5. The parameters are shown in Table 1.

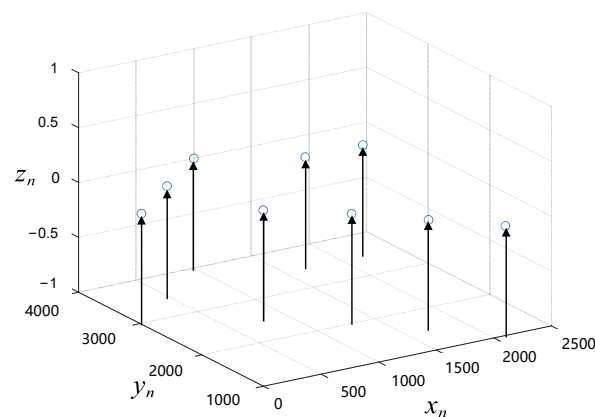


Figure 5. Wind farm layout.

Table 1. Parameters of wind farm layout.

Wind Turbine Order Number n	x_n (m)	y_n (m)	z_n (m)
1	10	3000	0
2	500	3500	0
3	800	2500	0
4	1000	4000	0
5	1300	2000	0
6	1700	1500	0
7	1700	3500	0
8	2100	1000	0
9	2200	3500	0

In addition, all wind turbines in the wind farm are of the same type, and the related parameters are shown in Table 2.

Table 2. Parameters of wind turbines.

Parameter	Value
Rotor diameter D	70 m
Hub height z_{hub}	65 m
Thrust coefficient C_T	0.705
Cut – in wind speed v_{in}	3.5 m/s
Rated wind speed v_r	13.5 m/s
Cut – out wind speed v_{out}	25 m/s
Rated power p_r	1700 kW
Rotor power Coefficient C_p	0.28

5.1.1. Under Different Wind Speeds

We consider the power of a wind farm under a single wind direction and different wind speeds. The wind direction is 0° (along the positive x -axis), and the wind speed ranges from 1 m/s to 32 m/s with intervals of 0.5 m/s. Other environmental parameters include the following: the wind speed reference height $z_{\text{ref}} = 65$ m, the air density $\rho = 1.225$ kg/m³, the turbulence intensity $k_y = k_z = 0.1$ and the wind shear index $\alpha = 0.15$. The power of the wind farm is shown in Figure 6. The following was found:

1. The power of wind farms under different wind speeds basically conforms to their variation law with wind speed;

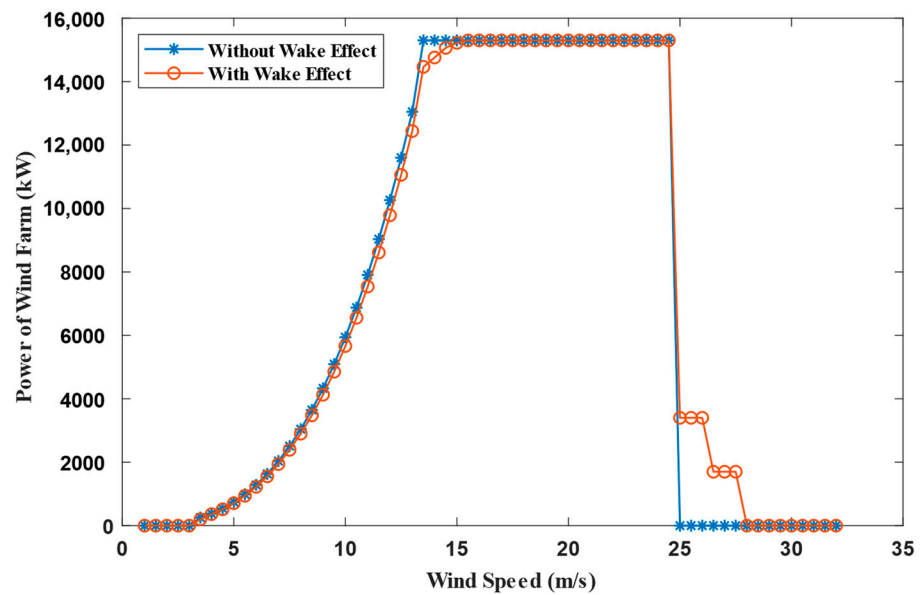


Figure 6. The power of a wind farm under different wind speeds.

When the wind speed is lower than a v_{in} of 3.5 m/s, the power of the wind farm is 0. When the wind speed gradually increases from 3.5 m/s, the power of the wind farm increases accordingly. When the wind speed reaches a v_r of around 13.5 m/s, the power of the wind farm remains stable. When the wind speed continues to increase to a v_{out} of 25 m/s or above, the power generated by the wind farm becomes 0 again. This is because the wind speed has reached the wind turbine cut-out wind speed, and in order to protect the equipment from damage, the wind turbines will stop generating power.

2. The power output of wind farms exhibits noticeable differences when the influence of wake is considered. This is especially pronounced when the wind speed approaches the rated wind speed and when it exceeds the cut-out wind speed.

The reason for this difference can be as follows:

When the wind speed increases to v_{in} , the upwind WT reaches v_{in} , while the downwind WT affected by the wake has not yet reached v_{in} , only the upwind WT starts generating electricity, and other downwind WT_s have not yet started. As the wind speed continues to increase, the amount of WT_s reaching v_{in} increases accordingly, increasing the power of the wind farm. However, the power of downwind WT_s is still lower than that without considering the wake effect. This is due to the fact that the wind speed of the downstream wind turbines is lower than the ambient wind speed due to the wake effect, resulting in lower power generation than without the wake effect. Therefore, when considering the wake effect, the power of the wind farm is always lower than when not considering the wake effect.

When the wind speed reaches v_r , the upwind WT reaches v_r , while the downwind WT_s affected by the wake has not yet reached v_r . As the wind speed continues to increase, all the downwind WT_s reach v_r , there is no difference in the power generated by the wind farm with or without considering wake effect. As the wind speed continues to increase, the downwind WT_s under the influence of the wake can still reach above v_r , and those downwind WT_s can also generate at its rated power.

Similarly, when the wind speed reaches v_{out} , the upwind WT reaches v_{out} and stops running, while the downwind WT₇ and WT₉ affected by the wake have not yet reached v_{out} and continued generating electricity. With the gradual increase in ambient wind speed, the wind speed of downwind WT₇ reaches the cut-out wind speed preferentially, while the wind speed of downwind WT₉ still does not reach the cut-out wind speed due to more influence from the wake effect. As the wind speed continues to increase, all the downwind WT_s reach v_r , there is no difference in the power generated by the wind farm with or

without considering wake effect. As the wind speed continues to increase, the downwind WT_5 under the influence of the wake can still reach above v_r , and those downwind WT_5 can also generate at its rated power.

5.1.2. Under Different Wind Directions

We consider the power of a wind farm under a single wind speed and different wind directions. The wind speed is 12 m/s, and the wind direction is in the range of 0° to 360° , with intervals of 45° . The other environmental parameters are the same as those shown in 5.1.1. The power of the wind farm is shown in Figure 7. The following can be found:

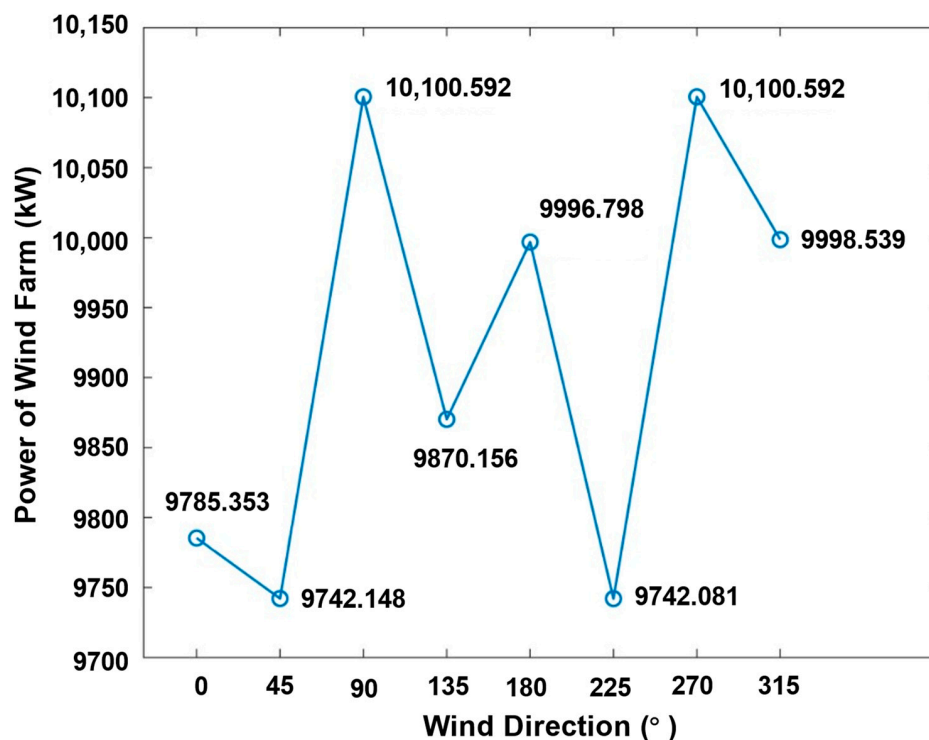


Figure 7. The power of the wind farm under different wind directions.

There are significant differences in the power of the wind farm in different wind directions. Under the eight wind directions, the power of the wind farm in descending order is $90^\circ = 270^\circ > 315^\circ \approx 180^\circ > 135^\circ > 0^\circ > 45^\circ \approx 225^\circ$. The wake influence between wind turbines varies in different wind directions, as shown in Figure 8. Wind farms with similar wake influences have similar power.

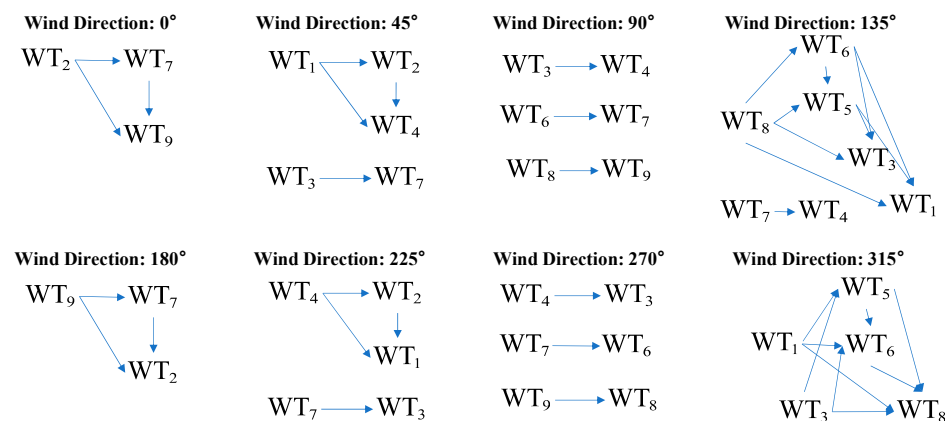


Figure 8. The wake influence between wind turbines under different wind directions.

At 90° and 270° , the wake influences of the wind farm are symmetrical, and the power generated by the wind farm is equal.

At 45° and 225° , WT_3 and WT_7 are symmetrical, WT_1 , WT_2 and WT_4 are approximately symmetrical because their positions are approximately in a straight line and the distance between WT_1 and WT_2 is approximately equal to the distance between WT_2 and WT_4 ; thus, the power of the wind farm is similar under the two wind directions 45° and 225° .

At 0° and 180° , although the influence relationships of WT_s are symmetrical, the intensity of wake influence is different; thus, the power of the wind farm is different under the two wind directions.

5.2. Belief Reliability of Wind Farm with Wind Speed Uncertainty

To present the belief reliability results based on the modeling method we proposed, a conventional wind distribution is utilized, followed by a comparison of the outcomes under wind distributions with varying degrees of dispersion.

5.2.1. Wind Farm Belief Reliability under Classical Wind Distribution

We consider the annual power generation of a wind farm under multiple wind directions and multiple wind speeds, which is a classical wind distribution used in [30–34]. The wind speeds are 8 m/s, 12 m/s and 17 m/s, the wind direction is in the range of 0° to 360° with intervals of 10° , and the frequency of each wind speed and direction are shown in Figure 9. The other environmental parameters are the same as those shown in Section 5.1.1.

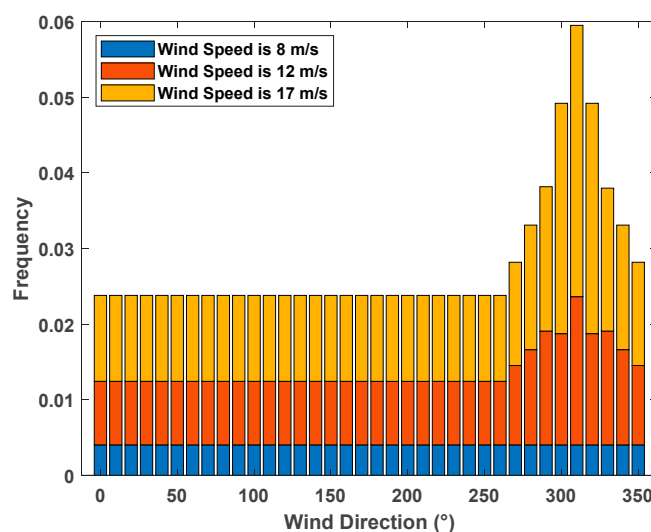


Figure 9. A classical wind distribution.

For the uncertainty of wind speed, to simplify the calculation and reduce the sampling dimension while keeping the sum of the three wind speeds unchanged, we considered that the first two wind speeds follow a two-dimensional normal distribution:

$$v \sim N(\mu, \Sigma), \quad (27)$$

$$\text{where } \mu = (8, 12), \Sigma = \begin{bmatrix} 0.3 & 0 \\ 0 & 0.3 \end{bmatrix}.$$

Here, we conducted 200 simulation samples. In each sample, the sum of the three wind speeds remained 37 and the frequency remained unchanged. The requirement of wind farm power generation is as follows: $E_{th} = 1.0 \times 10^{11}$ kWh. The belief reliability of the wind farm is 0.69.

5.2.2. Reliability Comparison with Different Dispersion Degrees of Wind Distribution

To compare the wind farm belief reliability under different dispersion degrees of wind distribution, we calculated the results under four other dispersion degrees of wind following different two-dimensional normal distribution. Still, the expected value in the two-dimensional normal distribution is $\mu = (8, 12)$, and the covariance matrices are $\Sigma = \begin{bmatrix} 0.1 & 0 \\ 0 & 0.1 \end{bmatrix}$, $\Sigma = \begin{bmatrix} 0.2 & 0 \\ 0 & 0.2 \end{bmatrix}$, $\Sigma = \begin{bmatrix} 0.4 & 0 \\ 0 & 0.4 \end{bmatrix}$ and $\Sigma = \begin{bmatrix} 0.5 & 0 \\ 0 & 0.5 \end{bmatrix}$.

Figures 10 and 11 present the frequency histogram of the performance margin and the belief reliability results, and the following can be found:

1. The uncertainty of the wind farm performance margin is positively correlated with the uncertainty of wind speed.

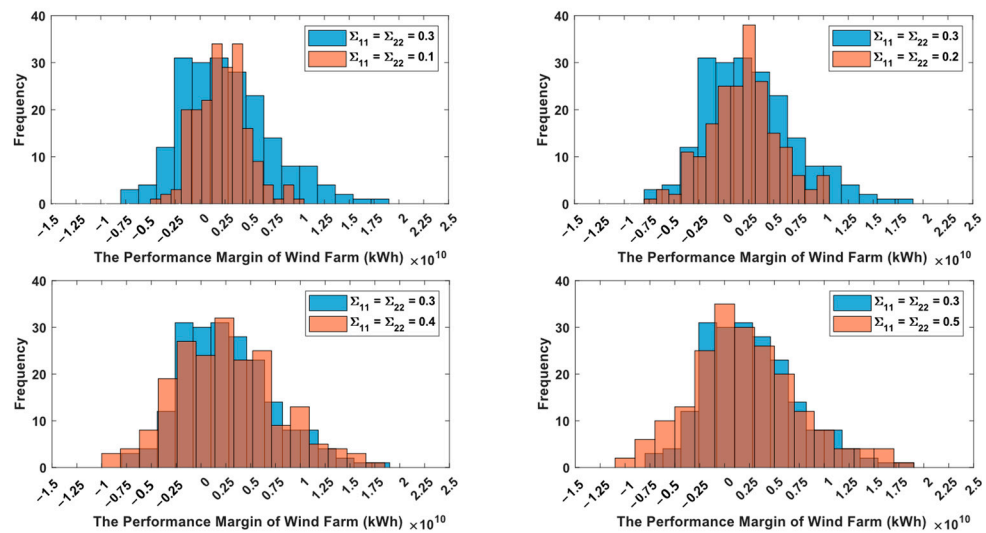


Figure 10. Frequency histogram of wind farm performance margin.

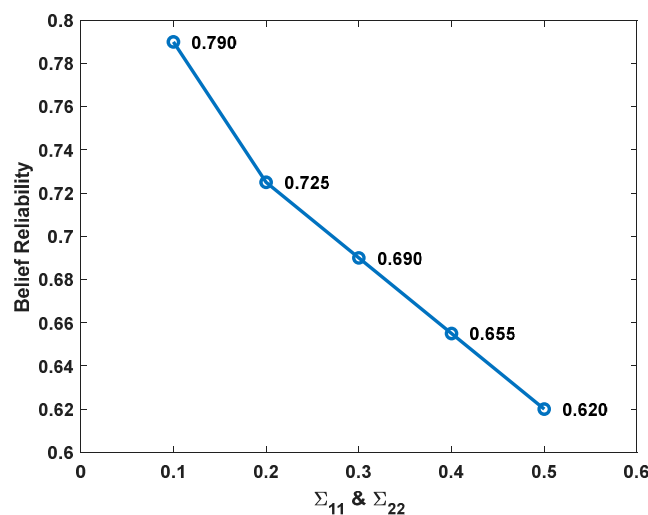


Figure 11. Belief reliability under different dispersion degrees of wind distribution.

As the variance of wind speed increases, both the dispersion of the wind speed and the performance margin also increase. Under a relatively dispersed wind distribution, although there are higher performance margins, there are also more performance margins less than 0, and this indicates that the uncertainty of wind farm performance margin is also greater.

- The belief reliability of a wind farm is positively correlated with the uncertainty of wind speed.

With the increased variance of wind speed, the belief reliability of wind farms decreases. This indicates that the greater the dispersion of wind speed, the greater the uncertainty of the performance margin, the lower belief reliability.

These trends regarding the relationship between wind speed uncertainty and both performance margin and belief reliability can reflect the actual patterns.

5.3. Comparison of Belief Reliability Considering HHWS, REWS and 2D-REWS

First, to provide a more intuitive explanation of the difference between HHWS, REWS and 2D-REWS, we illustrated three representative situations. Figures 4 and 12 show the three-positional relationship between the upwind turbine wake circle (the yellow one, abbreviated as C_{up} in the following) and the rotor circle of the downwind turbine (the transparent one, abbreviated as C_{down} in the following).

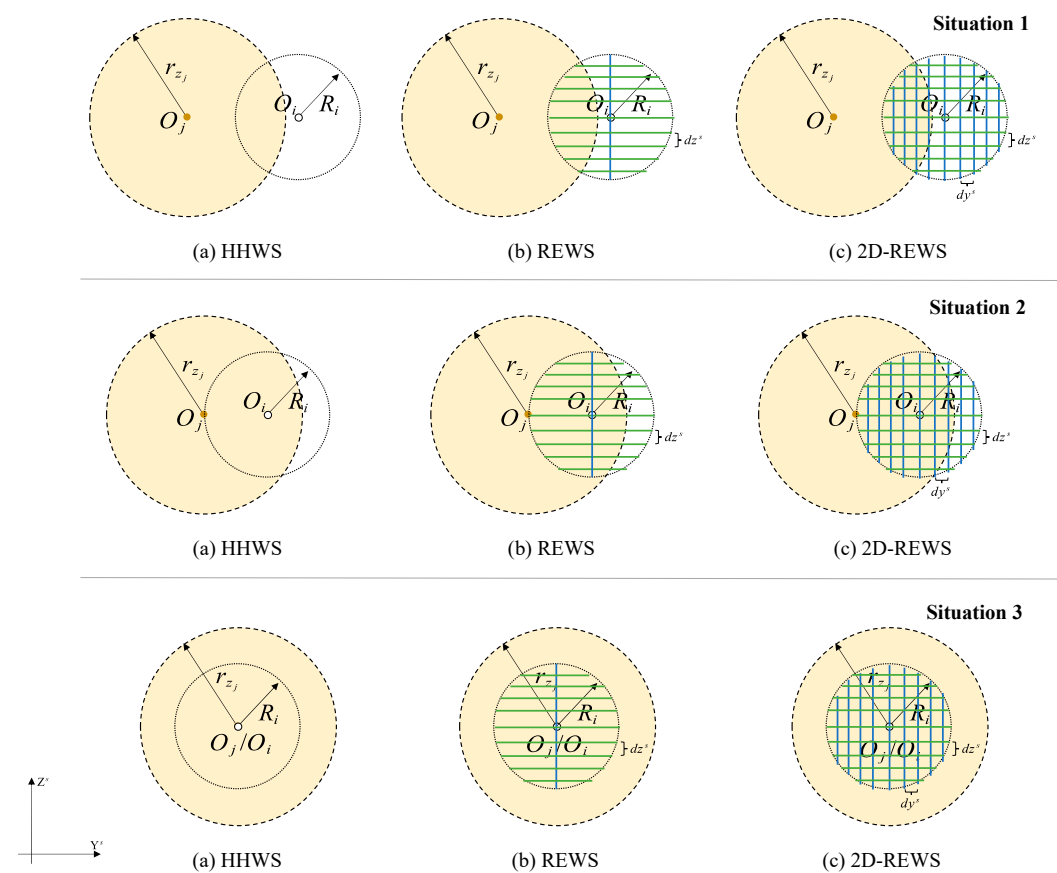


Figure 12. Diagram of different methods for representing the speed of the wind turbine.

According to HHWS, the wind speed of the center of C_{down} (denoted by O_i in (a) of Situation 1/2/3 in Figure 12) represents the speed of the whole downwind turbine. When O_i is outside C_{up} , the entire wind turbine will be considered unaffected by the wake, such as in the case of Situation 1 (a), where the wind speed is overestimated; when O_i is inside C_{up} , the entire wind turbine will be considered affected by the wake, such as in the case of Situation 2 (a), where the wind speed is underestimated; and when the centers of C_{up} and C_{down} overlap, the wake effect far from the center is lower than that near the center, such as in the case of Situation 3 (a), where the wind speed is underestimated.

According to REWS, the wind speed at different heights on the line perpendicular to the center of C_{down} (denoted by the blue line in (b) of Situation 1/2/3 in Figure 12) represents the speed at different heights of the downwind turbine, and the equivalent

wind speed is calculated using Equation (18). When the blue line is totally outside C_{up} , the entire wind turbine will be considered unaffected by the wake, such as in the case of Situation 1 (b), where the wind speed is overestimated; when the blue line is totally inside C_{up} , the entire wind turbine will be considered affected by the wake, such as in the case of Situation 2 (b), where the wind speed is underestimated; when the centers of C_{up} and C_{down} overlap, the wake effect far from the blue line is lower than that near the blue line, such as in the case of Situation 3 (b), where the wind speed is underestimated.

According to discretization 2D-REWS method, the wind speed of every intersection point of blue and green lines in C_{down} are used to calculate the equivalent wind speed, and there is no situation where the wind speed is underestimated or overestimated based on the continuous 2D-REWS method (Equations (19) and (20)).

Then, to analyze the wind farm belief reliability when using different methods for representing the speed of the wind turbine, we calculated the belief reliability results considering HHWS, REWS and 2D-REWS of three different wind farm layouts.

We consider the reliability of the wind farm under a single wind speed and single wind direction. The wind speed is 12 m/s, the wind direction is 0° . The relation between WTs is shown in the first subfigure in Figure 8. The rotor circles and wake circles of WT₂, WT₇, and WT₉ are all concentric circles.

Wind farm B is a control group whose layout is the same as that shown in Section 5.2.1. The layouts of wind farms A and C are changed. To ensure that the qualitative relationship between the upwind and downwind turbines remains unchanged and only the quantitative influence between WTs changes, the position of WT₉ is moved. The position of WT₉ in wind farm A is (2200,3400,0), and the position of WT₉ in wind farm C is (2200,3600,0).

The requirement of wind farm power generation is $E_{th} = 7.72 \times 10^{10}$ kWh. The other parameters are the same as those shown in Section 5.2.1. Here, we also conducted 200 simulation samples. The belief reliability of the wind farm is shown in Table 3. The following can be found.

Table 3. Belief reliability considering HHWS, REWS, and 2D-REWS.

Wind Farm Layout	HHWS	REWS	2D-REWS
A	0.845	0.840	0.830
B	0.780	0.785	0.790
C	0.840	0.840	0.835

Wind farm layouts A and C are similar to Situation 1, shown in Figure 8; thus, the wind speeds are overestimated. Wind farm layout B is similar to Situation 3, shown in Figure 8; thus, the wind speeds is underestimated. The values of belief reliability considering HHWS and REWS of wind farm layout A and C are both higher than that considering 2D-REWS, and the values of belief reliability considering HHWS and REWS of wind farm layout B are both lower than that considering 2D-REWS. The situation where belief reliability is underestimated and overestimated is the same as wind speed. In practice, more deviations will inevitably be introduced in reliability results when using HHWS or REWS. Thus, the belief reliability model considering 2D-REWS is more reasonable.

6. Conclusions

This paper proposes a new belief reliability modeling method for wind farms considering two-directional rotor equivalent wind speeds. Several conclusions can be drawn from this paper:

1. Only based on the performance margin and its threshold of wind farms, the proposed belief reliability modeling method allows for reliability analysis without relying on wind turbine failure information.

2. A 2D-REWS model was introduced, which incorporates a power generation model to enable belief reliability analysis that accounts for variations in wind speed across different heights and widths of wind turbines.
3. Numerical examples demonstrate that the variation of wind farm power with wind speed and direction is consistent with the actual patterns, the uncertainties in performance margin and belief reliability of a wind farm are both positively correlated with uncertainties in wind speed, and the belief reliability model considering 2D-REWS is more reasonable.

Future research directions may include incorporating factors such as the degradation of individual wind turbines and additional sources of uncertainty into the belief reliability model for wind farms. Additionally, we are interested in exploring layout optimization models based on the concept of belief reliability specifically tailored to enhance overall performance.

Author Contributions: Conceptualization, S.L. and R.K.; methodology, S.L.; software, S.L.; validation, S.L., M.W. and T.Z.; formal analysis, S.L., M.W. and T.Z.; investigation, S.L.; resources, M.W. and R.K.; data curation, S.L.; writing—original draft preparation, S.L.; writing—review and editing, S.L. and T.Z.; visualization, S.L.; supervision, M.W. and R.K.; project administration, M.W. and R.K.; funding acquisition, R.K. and M.W. All authors have read and agreed to the published version of the manuscript.

Funding: This research was funded by the National Natural Science Foundation of China, grant number 62073009 and the Stable Supporting Project of Science & Technology on Reliability & Environmental Engineering Laboratory, grant number WDZC20220102.

Data Availability Statement: All the data presented in the article do not require copyright. They are freely available from the authors.

Conflicts of Interest: The authors declare no conflicts of interest.

References

1. Hutchinson, M.; Zhao, F. *Global Wind Report 2023*; Global Wind Energy Council: Sao Paulo, Brazil, 2023.
2. Karki, R.; Billinton, R. Reliability/cost implications of PV and wind energy utilization in small isolated power systems. *IEEE Trans. Energy Convers* **2001**, *16*, 368–373. [[CrossRef](#)]
3. Sulaeman, S.; Benidris, M.; Mitra, J.; Singh, C. A Wind Farm Reliability Model Considering Both Wind Variability and Turbine Forced Outages. *IEEE Trans. Sustain. Energy* **2017**, *8*, 629–637. [[CrossRef](#)]
4. Miryousefi Aval, S.M.; Ahadi, A.; Hayati, H. A novel method for reliability and risk evaluation of wind energy conversion systems considering wind speed correlation. *Front. Energy* **2016**, *10*, 46–56. [[CrossRef](#)]
5. Leite, A.P.; Borges, C.L.T.; Falcao, D.M. Probabilistic wind farms generation model for reliability studies applied to Brazilian sites. *IEEE Trans. Power Syst.* **2006**, *21*, 1493–1501. [[CrossRef](#)]
6. Nemes, C.; Munteanu, F. Reliability Consideration on Wind Farms Energy Production. In Proceedings of the 13th International Conference on Optimization of Electrical and Electronic Equipment, Brasov, Romania, 24–26 May 2012; pp. 183–187.
7. Kim, H.; Singh, C.; Sprintson, A. Simulation and Estimation of Reliability in a Wind Farm Considering the Wake Effect. *IEEE Trans. Sustain. Energy* **2012**, *3*, 274–282. [[CrossRef](#)]
8. Jiang, W.; Yan, Z.; Feng, D.H. A review on reliability assessment for wind power. *Renew. Sustain. Energy Rev.* **2009**, *13*, 2485–2494. [[CrossRef](#)]
9. Billinton, R.; Gan, L. Wind power modeling and application in generating adequacy assessment. In Proceedings of the IEEE WESCANEX 93 Communications, Computers and Power in the Modern Environment, Saskatoon, SK, Canada, 17–18 May 1993; pp. 100–106.
10. Kumar, S.; Saket, R.K.; Dheer, D.K.; Sanjeevikumar, P.; Holm-Nielsen, J.B.; Blaabjerg, F. Layout optimisation algorithms and reliability assessment of wind farm for microgrid integration: A comprehensive review. *IET Renew. Power Gener* **2021**, *15*, 2063–2084. [[CrossRef](#)]
11. Negra, N.B.; Holmstrom, O.; Bak-Jensen, B.; Sorensen, P. Aspects of relevance in offshore wind farm reliability assessment. *IEEE Trans. Energy Convers* **2007**, *22*, 159–166. [[CrossRef](#)]
12. Kang, R. *Belief Reliability Theory and Methodology*; Springer: Singapore, 2021.
13. Li, Y.; Chen, Y.; Zhang, Q.; Kang, R. Belief reliability analysis of multi-state deteriorating systems under epistemic uncertainty. *Inf. Sci.* **2022**, *604*, 249–266. [[CrossRef](#)]
14. Li, X.-Y.; Chen, W.-B.; Kang, R. Performance margin-based reliability analysis for aircraft lock mechanism considering multi-source uncertainties and wear. *Reliab. Eng. Syst. Saf.* **2021**, *205*, 107234. [[CrossRef](#)]

15. Wang, Y.J.; Kang, R.; Chen, Y. Belief reliability modeling for the two-phase degradation system with a change point under small sample conditions. *Comput. Ind. Eng.* **2022**, *173*, 108697. [[CrossRef](#)]
16. Liu, Z.; Wang, S.H.; Liu, B.; Kang, R. Change point software belief reliability growth model considering epistemic uncertainties. *Chaos Solitons Fractals* **2023**, *176*, 114178. [[CrossRef](#)]
17. Liu, Z.; Yang, S.K.; Yang, M.H.; Kang, R. Software Belief Reliability Growth Model Based on Uncertain Differential Equation. *IEEE Trans. Reliab.* **2022**, *71*, 775–787. [[CrossRef](#)]
18. Yang, Y.; Huang, S.Y.; Wen, M.L.; Chen, X.; Zhang, Q.Y.; Liu, W. Analyzing travel time belief reliability in road network under uncertain random environment. *Soft Comput.* **2021**, *25*, 10053–10065. [[CrossRef](#)]
19. Jipeng, W.; Qingyuan, Z.; Yuanzhu, Z.; Xiaomei, S. Reliability Analysis and Health Management of the Radar Range Based on Belief Reliability Theory. In Proceedings of the 4th International Conference on System Reliability and Safety Engineering (SRSE), Electr Network, Guangzhou, China, 15–18 December 2022; pp. 278–283.
20. Wagner, R.; Cañadillas, B.; Clifton, A.; Feeney, S.; Nygaard, N.; Poodt, M.; Martin, C.S.; Tüxen, E.; Wagenaar, J.W. Rotor equivalent wind speed for power curve measurement—Comparative exercise for IEA Wind Annex 32. *J. Phys. Conf. Ser.* **2014**, *524*, 012108. [[CrossRef](#)]
21. Choukulkar, A.; Pichugina, Y.; Clack, C.T.M.; Calhoun, R.; Banta, R.; Brewer, A.; Hardesty, M. A new formulation for rotor equivalent wind speed for wind resource assessment and wind power forecasting. *Wind Energy* **2016**, *19*, 1439–1452. [[CrossRef](#)]
22. Scheurich, F.; Enevoldsen, P.B.; Paulsen, H.N.; Dickow, K.K.; Fiedel, M.; Loeven, A.; Antoniou, I. Improving the Accuracy of Wind Turbine Power Curve Validation by the Rotor Equivalent Wind Speed Concept. In Proceedings of the Conference on Science of Making Torque from Wind (TORQUE), Munich, Germany, 5–7 October 2016.
23. Jeon, S.; Kim, B.; Huh, J. Study on methods to determine rotor equivalent wind speed to increase prediction accuracy of wind turbine performance under wake condition. *Energy Sustain. Dev.* **2017**, *40*, 41–49. [[CrossRef](#)]
24. Redfern, S.; Olson, J.B.; Lundquist, J.K.; Clack, C.T.M. Incorporation of the Rotor-Equivalent Wind Speed into the Weather Research and Forecasting Model’s Wind Farm Parameterization. *Mon. Weather Rev.* **2019**, *147*, 1029–1046. [[CrossRef](#)]
25. Ryu, G.H.; Kim, D.; Kim, D.-Y.; Kim, Y.-G.; Kwak, S.J.; Choi, M.S.; Jeon, W.; Kim, B.-S.; Moon, C.-J. Analysis of Vertical Wind Shear Effects on Offshore Wind Energy Prediction Accuracy Applying Rotor Equivalent Wind Speed and the Relationship with Atmospheric Stability. *Appl. Sci.* **2022**, *12*, 6949. [[CrossRef](#)]
26. Gao, X.X.; Li, B.B.; Wang, T.Y.; Sun, H.Y.; Yang, H.X.; Li, Y.H.; Wang, Y.; Zhao, F. Investigation and validation of 3D wake model for horizontal-axis wind turbines based on filed measurements. *Appl. Energy* **2020**, *260*, 114272. [[CrossRef](#)]
27. IEC 61400-12-1; Wind Energy Generation Systems—Part 12-1: Power Performance Measurements of Electricity Producing Wind Turbines. International Electrotechnical Commission: Geneva, Switzerland, 2017.
28. Smith, G.; Schlez, W.; Liddell, A.; Neubert, A.; Peña, A. Advanced wake model for very closely spaced turbines. In Proceedings of the European Wind Energy Conference, Athens, Greece, 27 February–2 March 2006; pp. 1–9.
29. Barber, S.; Chokani, N.; Abhari, R.S. Wind Turbine Performance and Aerodynamics in Wakes within Wind Farms. In Proceedings of the Europe’s Premier Wind Energy Event (EWEA 2011), Brussels, Belgium, 14–17 March 2011.
30. Mosetti, G.; Poloni, C.; Diviacco, B. Optimization of wind turbine positioning in large windfarms by means of a genetic algorithm. *J. Wind Eng. Ind. Aerodyn.* **1994**, *51*, 105–116. [[CrossRef](#)]
31. Grady, S.A.; Hussaini, M.Y.; Abdullah, M.M. Placement of wind turbines using genetic algorithms. *Renew. Energy* **2005**, *30*, 259–270. [[CrossRef](#)]
32. Huang, H.-S. Efficient hybrid distributed genetic algorithms for wind turbine positioning in large wind farms. In Proceedings of the 2009 IEEE International Symposium on Industrial Electronics, Seoul, Republic of Korea, 5–8 July 2009; pp. 2196–2201.
33. Parada, L.; Herrera, C.; Flores, P.; Parada, V. Wind farm layout optimization using a Gaussian-based wake model. *Renew. Energy* **2017**, *107*, 531–541. [[CrossRef](#)]
34. Tao, S.Y.; Xu, Q.S.; Feijoo, A.; Zheng, G.; Zhou, J.M. Wind farm layout optimization with a three-dimensional Gaussian wake model. *Renew. Energy* **2020**, *159*, 553–569. [[CrossRef](#)]

Disclaimer/Publisher’s Note: The statements, opinions and data contained in all publications are solely those of the individual author(s) and contributor(s) and not of MDPI and/or the editor(s). MDPI and/or the editor(s) disclaim responsibility for any injury to people or property resulting from any ideas, methods, instructions or products referred to in the content.